

# Supporting Information

Huang et al. 10.1073/pnas.1300741110

## SI Materials and Methods

**Isolation, Culture, and Adenovirus Infection of Adult Rat Cardiomyocytes.** Male Sprague Dawley rats and spontaneously hypertensive rats (SHRs) (14 wk) were provided by the Centre for Experimental Animals at Peking University, China. Adult rat cardiomyocytes were enzymatically isolated. Cells were then cultured on dishes precoated with laminin (Sigma) in M199 medium (Sigma). After 1 h culture, cardiomyocytes were infected with adenovirus containing mitochondrial matrix-targeted photoactivatable green fluorescent protein (mtPAGFP) or outer membrane-targeted PAGFP-OMP25 or cytosolic PAGFP. Adenoviral vectors were packaged with the AdEasy XL Adenoviral System (Stratagene). Images were taken 60–72 h after infection.

**Confocal Microscopic Analyses.** Confocal imaging was carried out with a Zeiss LSM710 microscope with a 40 $\times$  oil-immersion objective. Cells were kept in a Heating Inset P S1 incubator at a constant temperature of 33–34  $^{\circ}$ C under 5% CO<sub>2</sub> (vol/vol). Regions of interest (ROIs) in cells expressing mtPAGFP or PAGFP-OMP25 or cytosolic PAGFP were photoactivated with an intense 405-nm laser scanning beam for designated durations. Time-lapse images were acquired by exciting at 488 nm and collecting the emission at >505 nm. Multitrack scanning was performed when cardiomyocytes were simultaneously loaded with tetramethyl rhodamine methyl ester (TMRM) (Invitrogen), when images were taken by exciting at 488 nm for PAGFP and 543 nm for TMRM, and collecting the emissions at 505–530 and >560 nm, respectively.

**Mitochondrial DNA Integrity Assay.** Mitochondrial DNA was quantified by the copy number ratio of integrated mtDNA with genomic DNA as previously reported (1). NADH dehydrogenase subunit 4 (ND4) was used to determine the integrated mtDNA, and the lipoprotein lipase (Lpl) gene for determining the genomic DNA. Primers were as follows: ND4-5', ATCGCACATGGCCTCACATC; ND4-3', TGTGTGTGAGGGTTGGAGGT; Lpl-5', GGATGGACGGTAAGAGTGATTC; Lpl-3', ATCCAAGGGTAGCAGACAGGT.

1. Zhao T, et al. (2012) Central role of mitofusin 2 in autophagosome-lysosome fusion in cardiomyocytes. *J Biol Chem* 287(28):23615–23625.

**Transmission Electron Microscopy.** Rat hearts were washed with saline and then perfused on a Langendorff apparatus with 3.5% glutaraldehyde in 0.1 M cacodylate buffer (pH 7.2) for fixation. These hearts were from previous experiments. Papillary muscles were excised and further treated as below. Isolated cardiac myocytes were fixed either in suspension immediately after isolation, or as soon as plated, or, after washing with PBS, incubation for 2–4 d with 2.5% glutaraldehyde in 0.1 M cacodylate (pH 7.2). All samples were postfixed with 2% osmium tetroxide in the same buffer for 1 h at 4  $^{\circ}$ C, treated en bloc with saturated uranyl acetate at room temperature, dehydrated, and embedded in Epon 812. Thin sections were either stained with lead citrate or double-stained with uranyl acetate and lead citrate and examined in a Philips 410 electron microscope (Philips Electron Optics) equipped with a Hamamatsu C4742-95 digital camera (Advanced Microscopy Techniques) or in a Tecnai 20 transmission electron microscope (FEI).

**Simulation of Kissing and Nanotunneling in the Cardiomyocyte.** One-dimensional numerical model consisting of 50 mitochondrial units 2  $\mu$ m in length were devised to represent an array of mitochondria along the longitudinal direction in an adult cardiomyocyte. In this model, each mitochondrion had a rate of  $p_1$  to kiss with its forward or backward neighbor. During kissing, these two mitochondria exchanged contents with a transfer index of  $\delta$ . In an event of nanotunneling, occurring at rate of  $p_2$ , content exchange occurred between a mitochondrion (at position 0) and any of its neighbors at positions  $-3$ ,  $-2$ ,  $2$ , and  $3$  with equal probability, bypassing its immediate neighbors at positions  $-1$  and  $1$ . The optimal values for the three model parameters,  $p_1$ ,  $p_2$ , and  $\delta$ , were determined by nonlinear (least-square error) fitting of Monte Carlo simulation results to the experimental data shown in Fig. 5D.

**Statistics.** Digital image processing and analysis were performed with IDL software (Research Systems) and custom-devised algorithms. Statistical data are expressed as mean  $\pm$  SEM, and Student  $t$  test was applied to determine the significance of the difference. A value of  $P < 0.05$  was considered statistically significant.

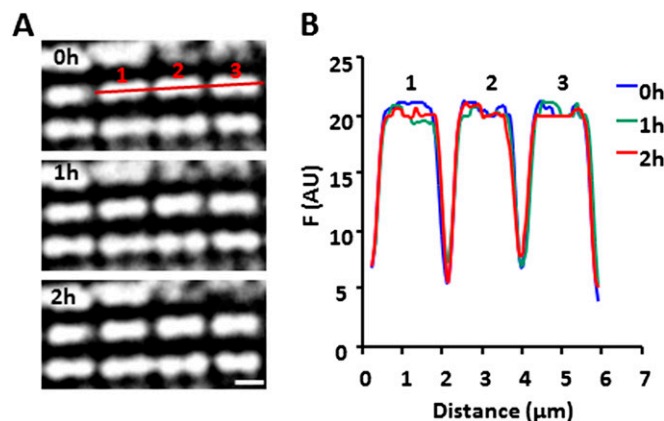
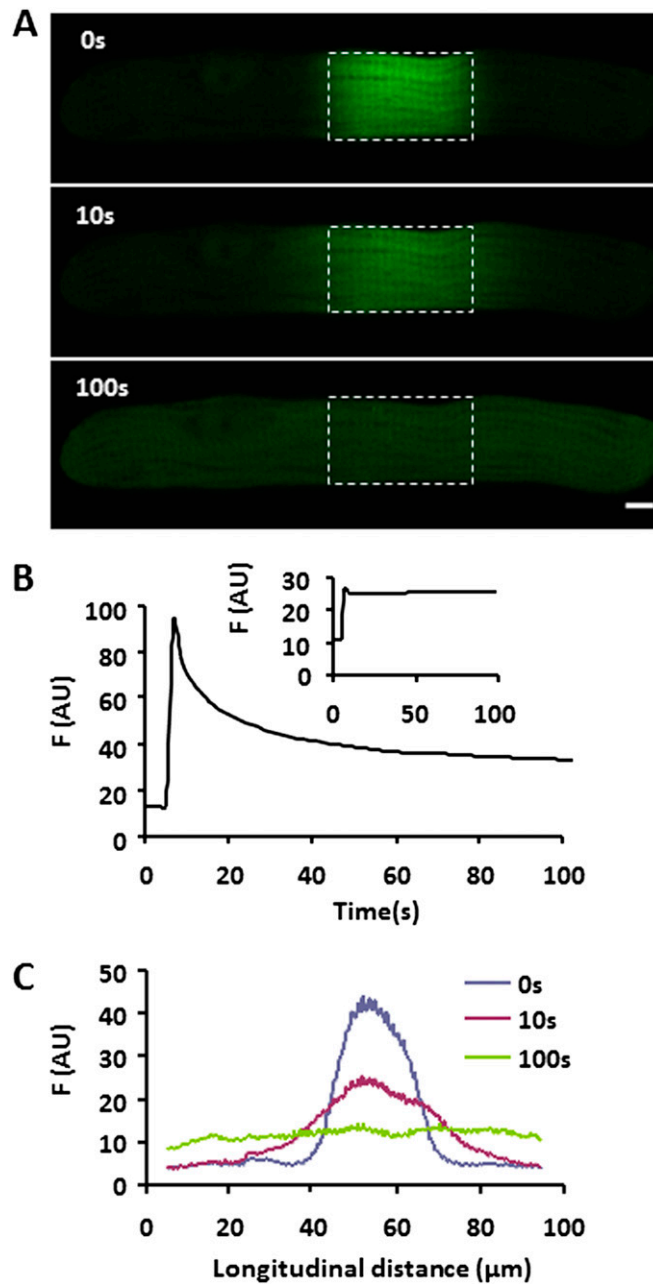
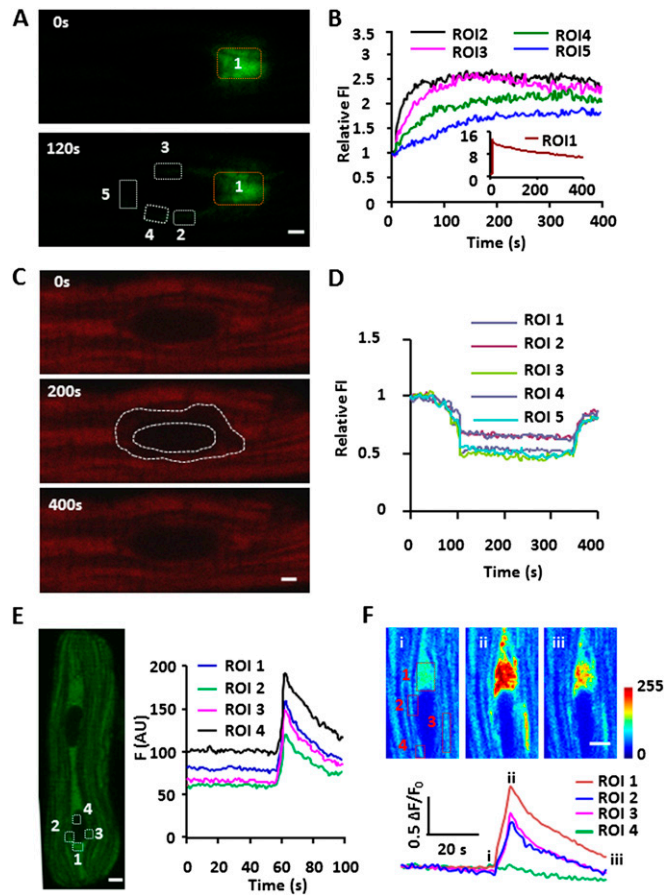


Fig. S1. Analysis of motility of interfibrillar mitochondria in adult rat cardiomyocytes. (A) Representative confocal images of cardiomyocytes stained with TMRM. (B) Fluorescent traces showing no movement of mitochondria as indicated in A for 2 h.



**Fig. S2.** Fast diffusion of PAGFP in the cytosol. (A) Sequential confocal images of a cardiomyocyte transfected with adeno-PAGFP after photoactivation. (Scale bar: 5  $\mu\text{m}$ .) (B) Time course of local PAGFP fluorescence from the photoactivated region in A. *Inset* shows total PAGFP fluorescence intensity from the whole cell. (C) Distribution of PAGFP fluorescence intensity along the cell length at different time points after photoactivation.



**Fig. 53.** Mitochondrial communication in the perinuclear area. (A) Rapid propagation of mtPAGFP signal in the mitochondrial network encircling the nucleus. The brown dashed box delimits the area of photoactivation. (B) Time course of local fluorescence intensity in boxed regions of interest (ROIs) in A. Data for the photoactivated region (ROI1) is shown as an *Inset*. (C) Synchronous mitochondrial membrane potential depolarization followed by uniform repolarization in the perinuclear zone as in A. The dashed lines delimit the boundary of the participating mitochondrial network (C). (Scale bar: 2  $\mu\text{m}$ .) (D) Time course of the perinuclear mitochondrial membrane potential oscillation shown in C. Similar results were obtained from 13 cardiomyocytes. (E and F) Synchronous mitochondrial flashes that envelope the nucleus completely (E) or partially (F) in cardiomyocytes expressing the superoxide biosensor mt-cpYFP, suggestive of a continuum for the interconnectivity of perinuclear and internuclear mitochondria. (Scale bar: 5  $\mu\text{m}$ .)

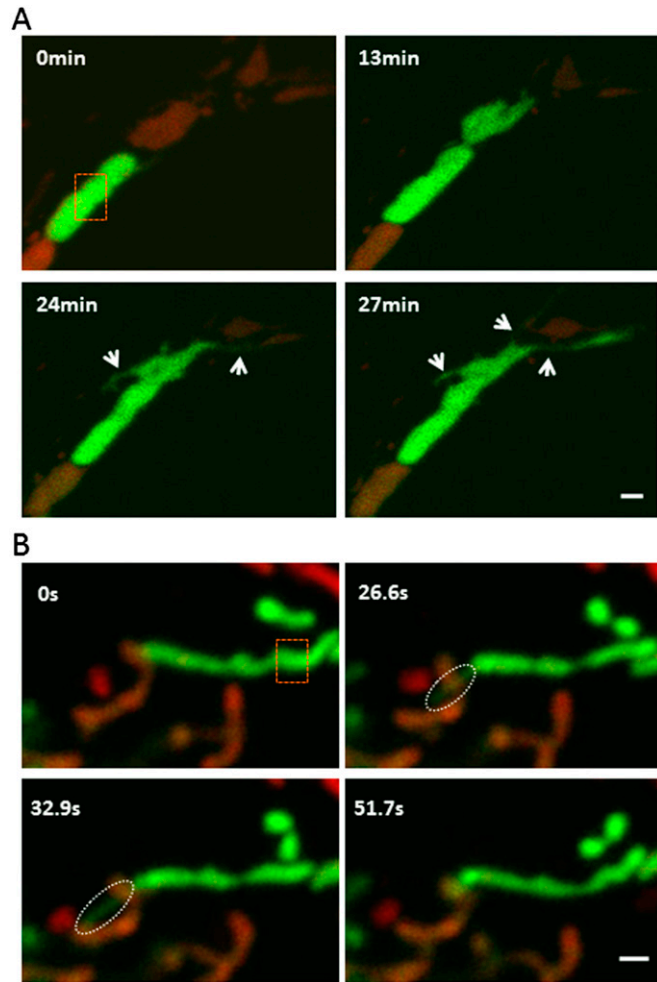


**Fig. 54.** Mitochondrial nanotunneling in neonatal cardiomyocytes and HeLa cells. (A) Mitochondrial nanotunneling in a neonatal cardiomyocyte. The arrows indicate the extending nanotubule-like structure. Note the transfer of mtPAGFP fluorescence. Region enclosed by the brown dashed line indicates photoactivated area. (Scale bar: 2  $\mu\text{m}$ .) (B) Mitochondrial nanotunneling in a HeLa cell. Regions in white elliptical dashed line indicate the extending nanotubule-like structure. Region enclosed by the brown dashed line indicates photoactivated area. (Scale bar: 1  $\mu\text{m}$ .) Green, mtPAGFP; red, TMRM.

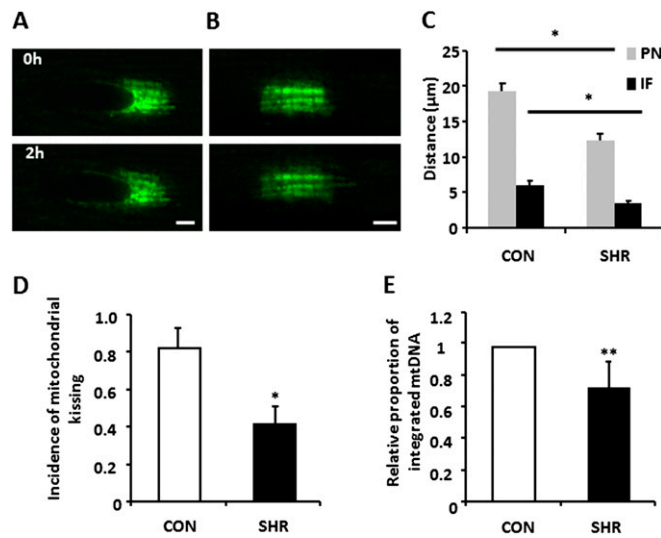
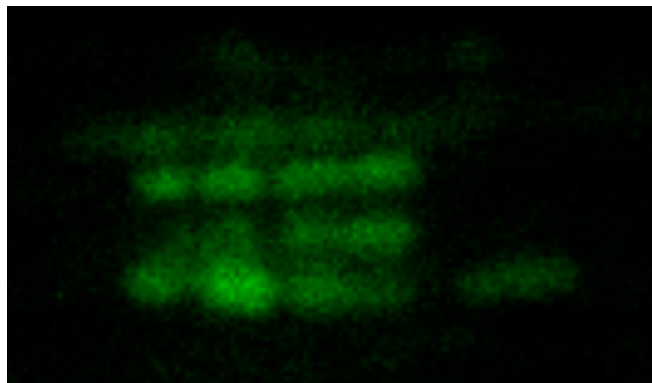


**Fig. S5.** Impaired mitochondrial communication in cardiomyocytes from SHR heart. (A and B) Representative confocal images of mtPAFGP signal immediately or 2 h after photoactivation, in perinuclear (A) and interfibrillar mitochondria (B) in cardiomyocytes from SHR heart. (Scale bars: 5  $\mu\text{m}$ .) (C) Travel distance of mtPAFGP signal 2 h after photoactivation, in mitochondria in the perinuclear (PN) and interfibrillar (IF) areas, from SHR and control cardiomyocytes. (D) Incidence of mitochondrial kissing in SHR and control hearts immediately after photoactivation of a  $4.9 \mu\text{m} \times 4.9 \mu\text{m}$  rectangular area recorded at one frame every 3 s for 10 min. (E) Change of integrated mtDNA to nuclear DNA ratio in SHR relative to control hearts. \* $P < 0.05$ ; \*\* $P < 0.01$  vs. control.  $n \geq 4$  pairs of control and SHR rats aged 14 wk.

**Table S1. TEM analysis of mitochondrial nanotubules in cardiomyocytes**

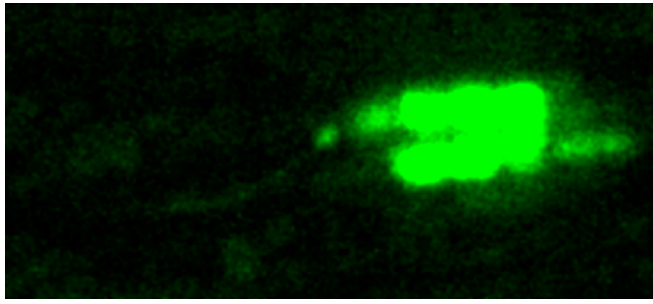
Cell status	Mitochondria with nanotubules, %	Disconnected nanotubules, %
Freshly isolated and fixed cells	5	1.5
Freshly isolated and plated cells	3	7
Cells cultured for 3 d	5	5

Numbers are percentage of total mitochondria without counting disconnected nanotubules. In total, 1,539–2,976 mitochondria from 18–24 cells in each group were counted.



**Movie S1.** Mitochondrial kissing.

[Movie S1](#)



**Movie S2.** Mitochondrial nanotunneling.

[Movie S2](#)